16. Кузнецов М. А. Термоэкономический анализ теплонасосной сушильной установки. *Проблемы машиностроения*. 2012. Т. 15. № 1. С. 36–42.
17. Kuznetsov M., Kharlampidi D., Tarasova V., Voytenko E. Thermoeconomic optimization of supercritical refrigeration system with the refrigerant R744 (CO_2). *Eastern-European J. Enterprise Technologies*. 2016. Vol. 6. No. 8 (84). – P. 24–32. https://doi.org/10.15587/1729-4061.2016.85397
18. Morandin M., Mercangöz M., Hemrle J., Marechal F., Favrat D. Thermoeconomic design optimization of a thermoelectric energy storage system based on transcritical CO_2 cycles. *Energy*. 2013. Vol. 58. P. 571–587. https://doi.org/10.1016/j.energy.2013.05.038
19. Lachner Jr. B. F., Nellis G. F., Reindl D. T. The commercial feasibility of the use of water vapor as a refrigerant. *Int. J. Refrigeration*. 2007. Vol. 30. No. 4. P. 699–708. https://doi.org/10.1016/j.ijrefrig.2006.09.009
20. Гохштейн Д. П. Современные методы термодинамического анализа энергетических установок. М.: Энергия, 1969. 368 с.
21. Энергетика: история, настоящее и будущее: в 5-ти т. Т. 3. Развитие теплоэнергетики и гидроэнергетики (под ред. В. Н. Клименко, Ю. А. Ландау, И. Я. Сигала). К.: Лира, 2011. 400 с.

DOI: https://doi.org/10.15407/pmach2019.02.031

UDC 621.81

EXPERIMENTAL STRENGTH ANALYSIS OF VARIABLE STIFFNESS WAFFEL-GRID CYLINDRICAL COMPARTMENTS PART 2. Analysis Results

[1] Maksim A. Degtyarev
maxim.dv@gmail.com

[1] Vitaliy G. Danchenko

[1] Artem V. Shapoval
artemshapoval7@gmail.com

[2] Konstantin V. Avramov
kvavr@kharkov.ua
ORCID: 0000-0002-8740-693X

[1] Yuzhnoye State Design Office,
3, Krivorizka str., Dnipro, 49008, Ukraine

[2] A. Podgorny Institute of Mechanical Engineering Problems of NASU,
2/10, Pozharsky str., Kharkiv, 61046, Ukraine

This paper presents the results of the experimental analysis of the stress-strain state of the variable stiffness tail compartment (section) designed by the Yuzhnoye Design Bureau. Equivalent compressive forces in the cross-sections of the tail compartment without the transport-erector support are analyzed. It is established that the calculated and experimental compressive forces are extremely close. Deformations in the tail compartment were measured where resistance strain gages were installed. For the measurement of displacements, displacement gauges were installed. The displacements were measured at six points. They were studied at maximum loading values corresponding to the fifth and sixth stages of loading. Axial movements are always negative, which indicates that the shell is compressed in the axial direction. The stress-strain state of the launch vehicle tail compartment was experimentally investigated. The circumferential normal stresses are several orders of magnitude smaller than the longitudinal ones. Therefore, the circumferential stresses were not investigated. The results of the experimental studies were compared with the numerical simulation data in the NASTRAN software package. The purpose of the simulation was to confirm the workability of the tail compartment under the loads that occur during operation. In other words, the design must withstand the actual loads without destruction and the appearance of plastic deformations. Special attention was paid to the zones that were directly under the brackets. The experimental results and numerical simulation data are close.

***Keywords**: stress-strain state of tail compartment, equivalent compressive forces, displacement measurements.*

Introduction

In the first part of this article [1], a technique for the experimental study of the strength of the launch vehicle (LV) tail compartment was developed. The tail compartment is a waffle-grid thin-walled structure, which consists of two shells. This part of the article presents the results of experimental studies based on the methodology developed in the first part.

Results of Experimental Analysis

Let us present the results of the experimental analysis of the stress-strain state (SSS) arising in the LV tail compartment. The loading diagram of the LV compartment is shown in Fig. 1. The equivalent compressive forces were investigated in the five different cross-sections designated as follows: VI – upper extreme (end) frame, V – beginning of the upper waffle-grid shell, IV – weld place between the lower and upper waffle-grid shells, III – beginning of the lower waffle-grid shell, II – cross-section on the tail compartment lower frame.

The results of the analysis of the compressive forces are given in Tables 1 and 2. Table 1 shows the equivalent compressive forces in the cross-sections of the tail compartment without the transporter-erector (TE) support. The first column of the table shows the cross-section number in which the compressive forces were investigated. The second column presents the calculated values of the compressive forces, which are realized during operation as part of the LV. The third and fourth columns show the results of the experimental analysis of the compressive forces, with the results obtained for the first and second loading cases (Fig. 3, [1]). As follows from Table 1, the design and experimental compressive forces are extremely close. Table 2 presents the results similar to those in Table 1, only for the case of loading the LV with the TE support.

Deformations in the tail compartment were measured where the resistive strain gauges were placed as shown in Fig. 4 [1] with the inverted letter T. Using Hooke's law, the circumferential stresses σ_y and longitudinal stresses σ_x [2] were recalculated from the values of longitudinal and circumferential deformations.

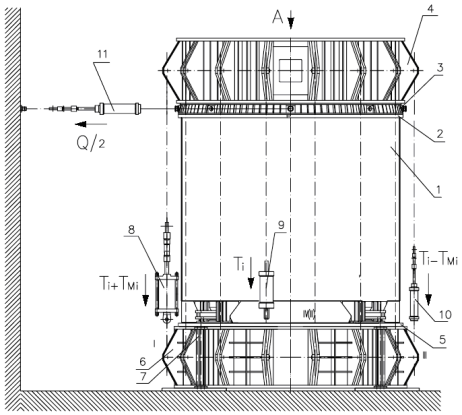

Fig. 1. Tail compartment installation diagram for experimental analysis

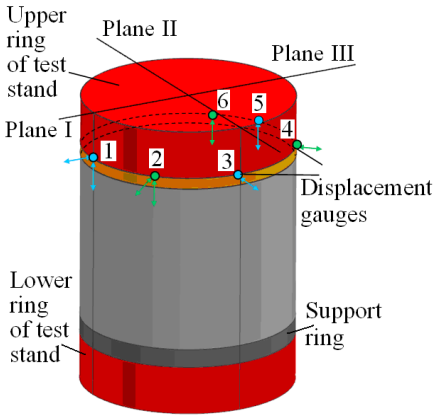

Fig. 2. Layout diagram of displacement gauges

Table 1. Equivalent compressive forces in the tail compartment cross- sections for the fully fueled LV resting on the launch pad without the TE support

Cross-section	Design load, tf (*f*=1.3)	Test load, tf	
		in plane I–III	at an angle of 45°
VI	559.389	562.479	564.719
V	560.836	566.763	569.012
IV	576.475	581.711	583.990
III	592.094	596.510	598.820
II	593.579	597.907	600.220

Table 2. Equivalent compressive forces in the tail compartment cross- sections for the fully fueled LV resting on the launch pad with the TE support

Cross-section	Design load, tf (*f*=1.3)	Test load, tf	
		in plane I–III	at an angle of 45°
VI	596.439	599.469	692.393
V	599.089	603.352	696.811
IV	611.441	616.915	712.220
III	625.831	630.330	727.481
II	624.737	631.602	728.919

To measure displacements, gauges were installed as shown in Fig. 2. The displacements were measured at six points. They were studied at maximum loading values corresponding to the fifth and sixth stages of loading. These loads are presented in the last columns of Tables 1–4 [1]. The results of measurements of the axial and radial displacements are given in Table 3. As follows from this table, the axial displacements are always negative, which indicates that the shell is compressed in the axial direction. The first column of Table 3 shows the numbers of the points presented in Fig. 2. The table shows the displacement projection measurements, which were carried out for the first and second cases of loading the tail compartment (Fig. 3, [1]).

The theoretical calculations, which were carried out for comparison with the experimental data, are presented in Table 4. It shows both the maximum displacements obtained experimentally and the calculated values. The last line of the table shows the difference between the experimental and calculated values in percent. In most cases, the relative error is in the range of permissible values. In this case, the error is 27.8%.

Now let us present the results of the experimental analysis of the LV tail compartment SSS. As follows from the experimental analysis, under the loading conditions shown in Fig. 3 [1], the circumferential normal stresses are several orders of magnitude smaller than the longitudinal ones. Therefore, the circumferential stresses are not investigated.

The results of the experimental analysis of the longitudinal stresses are presented in Figs. 3–6. Each of them shows the distribution of the longitudinal stresses for the three cross-sections denoted by numbers 1, 2, 3. These three layers of measurements are indicated in Fig. 4 [1] by an inverted letter T. Cross-section numbers are placed from top to bottom. Cross-section 1 is at the top, and cross-section 3 is at the bottom. Fig. 3 shows the distribution of the longitudinal stresses along the circumferential coordinate for the fully fueled LV resting on the launch pad without the TE support. The loads applied to the tail compartment correspond to loading stage 5. It is presented in Table 1 [1]. It is to be emphasized that these loads are applied in the plane I–III. Fig. 4 shows the distribution of the longitudinal stresses in the three cross-sections, with the distribution depending on the circumferential coordinate for the fully fueled LV resting on the launch pad with the TE support. The loads acting on the LV are presented in the last column of Table 2 [1]. These loads are applied in the plane I–III (Fig. 3).

The magnitudes of the maximum stresses for the case of loads with the TE support are greater than those for the case without it. As follows from Tables 3, 4 [1], in the case of the TE support, the magnitude of the longitudinal compressive force is greater.

Table 3. Results of measurements of maximum displacements

Point number	Direction of measurement	In-plane loading		Loading at an angle of 45°	
		Without TE support	With TE support	Without TE support	With TE support
		Displacements, mm			
1	Axial	-6.46	-6.19	-4.41	-5.64
	Radial	-3.59	-2.75	-2.36	-2.03
2	Axial	-5.91	-5.90	-6.03	-7.22
	Radial	-3.17	-2.19	-2.84	-2.30
3	Radial	-0.43	-0.10	-3.14	-3.04
4	Radial	3.35	2.73	0.34	0.39
5	Axial	-0.56	-1.82	-1.94	-3.33
6	Axial	-2.00	-2.87	-0.94	-2.54

Table 4. Comparison of the maximum experimental and calculated tail compartment displacements where the resistive strain gauges are installed

Type of data	Tail compartment loading in the plane I–III				Tail compartment loading at an angle of 45° from plane I to plane IV			
	Axial	Radial	Axial	Radial	Axial	Radial	Axial	Radial
	Without TE support		With TE support		Without TE support		With TE support	
Experimental values, mm	-6.46	-3.59	-6.19	-2.75	-6.03	-3.14	-7.22	-3.04
Calculated values, mm	-6.58	-3.37	-6.22	-3.81	-6.16	-3.70	-7.44	-2.75
Δ, %	1.82	6.12	0.48	27.8	2.11	15.13	2.95	9.53

Now let us consider the results of the SSS analysis for the second case of loading (Fig. 3, [1]). The results of the experimental analysis of the distribution of the longitudinal stresses in the three cross-sections of the tail compartment, with the distribution depending on the circumferential coordinate, for the fully fueled LV resting on the launch pad without the TE support are shown in Fig. 5. The loads acting on the tail compartment are given in the last column of Table 3 [1].

Fig. 6 shows the distribution of the longitudinal stresses in the three cross- sections, depending on the circumferential coordinate, for the fully fueled LV resting on the launch pad with the TE support. The loads acting on the LV are presented in the last column of Table 4 [1]. These loads are applied at an angle of 45º from plane I to plane IV (Fig. 3, [1]).

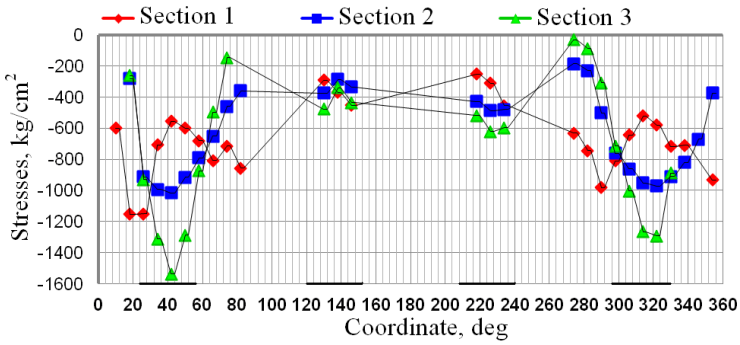

Fig. 3. Distribution of the longitudinal stresses in the cross-sections of the tail compartment for the fully fueled LV standing on the launch pad without the TE support

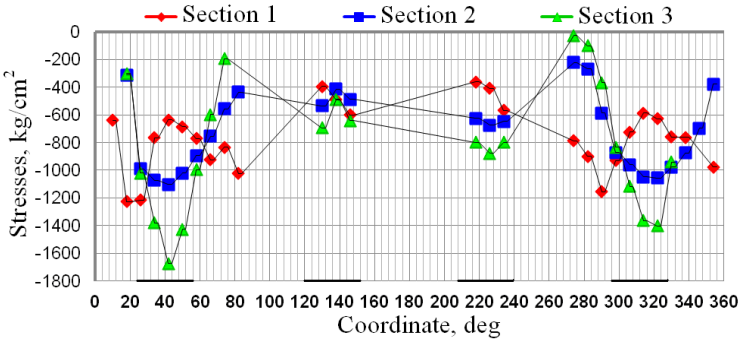

Fig. 4. Distribution of the longitudinal stresses in the cross-sections of the tail compartment for the fully fueled LV standing on the launch pad with the TE support

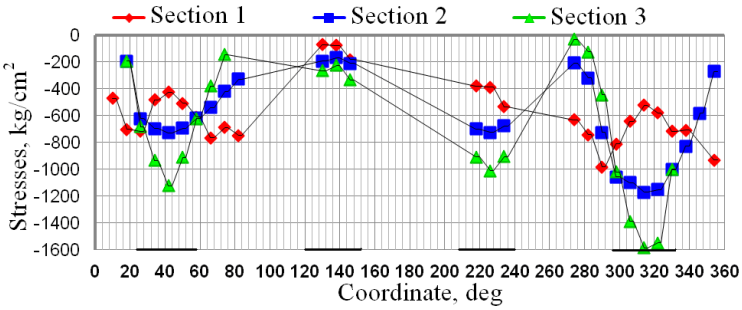

Fig. 5. Distribution of the longitudinal stresses in the cross-sections of the tail compartment for the fully fueled LV standing on the launch pad without the TE support

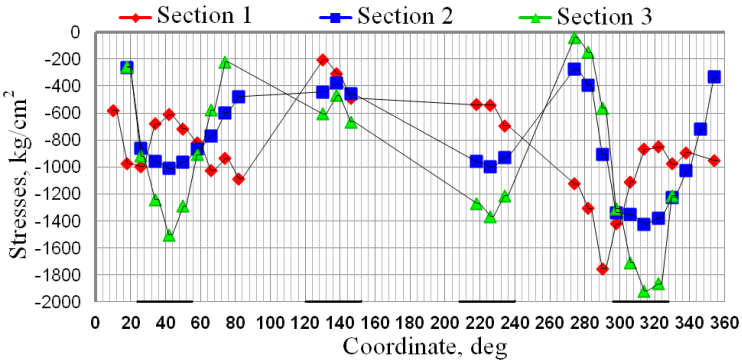

Fig. 6. Distribution of the longitudinal stresses in the cross-sections of the tail compartment for the fueled LV resting on the launch pad with the TE support

As follows from the results of the experimental analysis, in the above four cases of loading, the tail compartment, the magnitude of the longitudinal stresses is less than the yield strength of the material. Therefore, the tail compartment is in the area of elasticity.

Numerical Simulation of Stress State

In this section, results of the finite element simulation of the tail compartment SSS in the NASTRAN software package are presented. The purpose of the simulation was to confirm the performance of the tail compartment under the loads that occur during operation. In other words, the design must withstand the actual loads without destruction and the appearance of plastic deformations. Special attention was paid to the zones that were directly under the brackets and are marked with the signs (Y) and (Z) (Fig. 2 [1]). According to the results of the calculations, it was decided to increase the thickness of the load-carrying structure elements where the brackets are installed. Such reinforcements form the so-called load-carrying columns, whose widths match the brackets. During the calculations and trials, attention was paid specifically to these zones, so that plastic deformations were not observed in them [2].

The results of the simulation of the tail compartment SSS for the fully fueled LV resting on the launch pad without the TE support are shown in Fig. 6. The loads acting on the LV are in the plane I–III. These loads are given in the fifth column of Table 1 [1]. Fig. 7 shows the longitudinal stresses in the tail section. We emphasize that the tensile stresses are positive, and the compressive ones are negative. Fig. 7 presents the distribution of the longitudinal stresses in the tail compartment under the action of the loads describing the fully fueled LV resting on the launch pad, taking into account the TE support. The loads acting on the LV are related to the first loading case (Fig. 3 of [1]).

The values of the experimental SSS measurements were compared with the data of its numerical simulation in the NASTRAN software package. The results of this comparison are presented in Table 5, where the maximum longitudinal stresses occurring in the tail compartment are shown. The second line contains the experimental values of the longitudinal compressive stresses, and the third one gives the calculated values. The fourth line shows the relative error of the experimental and calculated values. So, the experimental and calculated results are close.

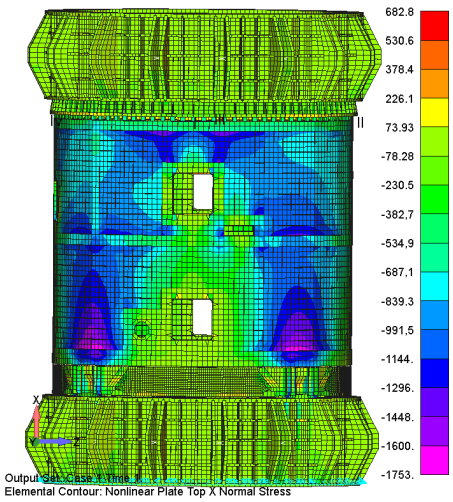

Fig.6. Tail compartment SSS under the action of design loads for the fully fueled LV resting on the launch pad without the TE support

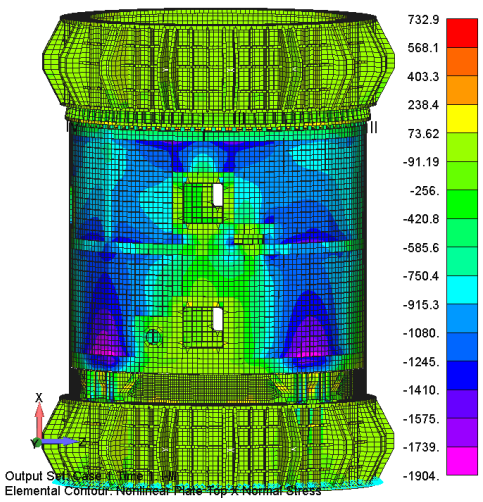

Fig. 7. Tail compartment SSS for the fully fueled LV resting on the launch pad with the TE support

Table 5. Maximum experimental and calculated longitudinal compressive stresses in the tail compartment

Types of data	Planes I–III		At an angle of 45° from plane I plane IV	
	Without TE support	With TE support	Without TE support	With TE support
Experimental data, kgf/cm^2	-1538	-1674	-1587	-1922
Calculated data, kgf/cm^2	-1598	-1738	-1797	-2072
Δ, %	3.75	3.68	11.68	7.23

Conclusions

The experimental studies of the tail compartment were carried out under the action of the maximum loads applied thereto when the fully fueled LV rested on the launch pad with or without the TE support. For each case, the loading of the tail compartment was implemented both in the TE plane and at an angle of 45° to this plane. Upon reaching 130 and 150% of the operational load, the loss of structure performance was not observed, which confirms the sufficient strength of the tail compartment. The tail compartment SSS analysis at maximum loading levels showed a fairly good closeness between the calculated and experimental parameters. The difference between the maximum experimental and calculated SSS parameters is from 3.75 to 11.68%. The maximum stresses in the tail compartment did not reach the yield strength of the material. Therefore, the material of the tail compartment is in the area of elasticity.

Upon testing, the tail compartment condition inspection confirmed the absence of defects in welded joints and residual deformations in the structure, as well as the compartment connectivity with the test technological rings.

References

1. Degtyarev, M. A., Danchenko, V. G., Shapoval, A. V., & Avramov, K. V. (2019). Experimental strength analysis of variable stiffness waffel-grid cylindrical compartments. Part 1. Experimental procedure. *Journal of Mechanical Engineering*, vol. 22, no. 1, pp. 33–36. https://doi.org/10.15407/pmach2019.01.033
2. Kobayasi, A. (1990). *Eksperimentalnaya mekhanika* [Experimental mechanics]. Moscow: Mir, 550 p. (in Russian).
3. Rabotnov, Yu. N. (1988). *Mekhanika deformiruyemogo tverdogo tela* [Mechanics of a deformable solid]. Moscow: Nauka, 710 p. (in Russian).

Received 12 July 2018

Експериментальний аналіз міцності вафельних циліндричних відсіків змінної жорсткості. Частина 2. Результати аналізу

[1] Дегтярев М. О. , [1] Данченко В. Г., [1] Шаповал А. В. , [2] Аврамов К. В.

[1] Державне підприємство «Конструкторське бюро «Південне» ім. М.К. Янгеля»,
49008, Україна, м. Дніпро, вул. Криворізька, 3

[2] Інститут проблем машинобудування ім. А.М. Підгорного НАН України,
61046, Україна, м. Харків, вул. Пожарського, 2/10

Подані результати експериментального аналізу напружено-деформованого стану хвостового відсіку змінної жорсткості, який спроектований в КБ "Південне". Аналізу піддавалися еквівалентні стискальні зусилля в поперечних перерізах хвостового відсіку без підтримки транспортно-інсталяційного агрегату. Встановлено, що розрахункові та експериментальні стискальні зусилля надзвичайно близькі. Вимірювання деформацій в хвостовому відсіку проводилося в місцях установлення тензорезисторів. Для вимірювання переміщень монтувалися датчики переміщень. Переміщення вимірювалися в шести точках. Вони досліджувалися за максимальних значень навантажень, що відповідають п'ятому та шостому етапам навантаження. Осьові переміщення завжди негативні, що свідчить про стиск оболонки в осьовому напрямку. Експериментально досліджувався напружено-деформований стан хвостового відсіку ракети-носія. Обводові нормальні напруження на декілька порядків менше поздовжніх. Тому обводові напруження не досліджувались. Результати експериментальних досліджень порівнювались з даними чисельного моделювання в програмному комплексі NASTRAN. Метою моделювання було підтвердження працездатності хвостового відсіку при навантаженнях, що виникають під час експлуатації. Іншими словами, конструкція повинна витримати діючі навантаження без руйнування і появи пластичних деформацій. Особлива увага приділялася зонам, які перебували безпосередньо під кронштейнами. Експериментальні результати і дані чисельного моделювання близькі.

Ключові слова: *напружено-деформований стан хвостового відсіку, еквівалентні стискальні зусилля, вимірювання переміщень.*

Література

1. Degtyarev M. A., Danchenko V. G., Shapoval A. V., Avramov K. V. Experimental strength analysis of variable stiffness waffle-grid cylindrical compartments. Part 1. Experimental procedure. *J. Mech. Eng*. 2019. Vol. 22. No. 1. P. 33–36. https://doi.org/10.15407/pmach2019.01.033
2. Кобаяси А. Экспериментальная механика. М.: Мир, 1990. 550 с.
3. Работнов Ю. Н. Механика деформируемого твердого тела. М.: Наука, 1988. 710 с.